# Green Synthesized Approach to Develop Tungsten Nanostructures for Biosensor Applications

**Oday Jawad Kadhim**

**Department of Physics, College of Science, Wasit University, Iraq.**

## Abstract

The current paper presents a novel green synthesis approach for developing tungsten oxide ($WO_3$) nanostructures using green apple extract as a natural reducing and capping agent. The synthesis method effectively produced monoclinic $WO_3$ nanostructures with well-controlled morphology and size distribution, exhibiting a mean diameter of 27.376 nm and crystallite sizes averaging 21.34 nm. XRD analysis confirmed the formation of pure-phase monoclinic $WO_3$, while FESEM revealed uniform quasi-spherical morphology. The FTIR spectroscopy demonstrated successful functionalization with biomolecules from the apple extract, and EDX confirmed the chemical composition with 75.82 wt % for tungsten, 18.17 wt % for oxygen, and 6.01 wt % for carbon. The synthesized nanostructures showed excellent potential for biosensor applications, demonstrating rapid response time (4.2 s), quick recovery (8.5 s), and high stability (± 2.3 % signal drift) in glucose sensing application.

**Keywords**: Green Synthesis, Tungsten Oxide Nanostructures, Apple Extract, Biosensor Applications, and Monoclinic $WO_3$

## 1. Introduction

Biosensors are analytical devices that convert biological responses into measurable signals. The emergence of nanotechnology has revolutionized biosensor development, particularly by tungsten-based materials [1]. Tungsten and its compounds (including tungsten carbide, oxide, and disulfide) are especially promising due to their unique properties. Unique properties include excellent electrical conductivity, high mechanical strength, high melting point, wear resistance, low thermal expansion, oxidation resistance, and biocompatibility

[2]. Traditional synthesis methods for tungsten nanostructures, such as chemical vapor deposition and thermal spraying, often require high temperatures, toxic chemicals, and expensive equipment. This has led to increased interest in "green synthesis" methods, which use natural resources like plant extracts and bacteria [3]. These environmentally friendly approaches are less toxic and more cost-effective than conventional methods, though they face some challenges with reproducibility and scalability [4].

At the nanoscale, tungsten materials exhibit enhanced properties compared to their bulk counterparts, including higher surface-to-volume ratios and improved catalytic activity. While bulk tungsten is biologically inert, its nanostructured form shows improved biocompatibility, making it suitable for biosensor applications. Recent research has demonstrated tungsten nanostructures' effectiveness of detecting various biomolecules in 25 biosensor applications documented since 2019. Notably, twelve of these applications achieved World Health Organization (WHO) detection limits, particularly in medical diagnostics for conditions like cancer, heart disease, and diabetes, as well as environmental monitoring of heavy metals and pesticides [5, 6].

Green synthesis methods are based on the principles that emphasize resource efficiency, waste reduction, and the use of benign solvents and catalysts [7]. These approaches are particularly valuable for biosensor applications, where biocompatibility is crucial since biological recognition elements can be sensitive to harsh chemical conditions. While green synthesis methods show great promise, ongoing research aims to address challenges in yield and purity levels to make these approaches more practical for commercial applications [8].

## 2. Materials and methods

The synthesis was carried out using tungsten (VI) chloride ($WCl_6$, 99.9 %, Sigma-Aldrich) as the metal precursor. Fresh green apples were purchased from a local market and thoroughly cleaned before use. All solutions were prepared using deionized water (18.2 MΩ·cm resistivity). Standard solutions of NaOH and HCl (analytical grade) were used for pH adjustment. Whatman No. 1 filter paper was used for filtration processes. All glassware used in the experiments was thoroughly cleaned with deionized water and dried before use.

## 2.1 The green apple extract preparation

The extract preparation process involved a 100 g of fresh green apples were thoroughly washed with deionized water and cut into small pieces. Pieces were boiled in a 500 mL of deionized water for 30 minutes at 80 °C. After cooling to room temperature, the mixture was filtered using filter paper to obtain a clear extract solution. The extract was stored at 4 °C until further use.

## 2.2 Tungsten nanostructure synthesis

A 0.5 Molar solution of tungsten (VI) chloride was prepared by dissolving the appropriate amount of $WCl_6$ in deionized water (0.198 g/mL). The solution was stirred continuously at room temperature until complete dissolution. 50 mL of the prepared green apple extract was added dropwise to 100 mL of the 0.5 M tungsten chloride solution under constant magnetic stirring at 60 °C. The pH of the reaction mixture was maintained at 7.0 using dilute NaOH as needed. The reaction was allowed to proceed for 2 hours, during which the color change from light yellow to dark brown indicated the formation of tungsten nanostructures. The resulting solution was centrifuged at 4,000 rpm for 15 minutes to collect the nanostructures. The precipitate was washed several times with deionized water and ethanol to remove any unreacted materials and impurities. The purified nanostructures were then dried in an oven at 60 °C for six hours to obtain the powder product. Then, the dried powder was calcined in a muffle furnace at 400 °C for two hours with a heating rate of 5 °C per minute under air atmosphere. This calcination step helps to remove any remaining organic materials from the apple extract and improves the crystallinity of the tungsten nanostructures.

## 2.3 Calcined nanostructures characterization

Calcined nanostructures were characterized by using XRD for crystal structure analysis (confirming the formation of crystalline tungsten phases), FESEM for morphological studies (showing particle size and distribution), and FTIR for identifying the functional groups present on the surface of the nanostructures. This green synthesis approach utilizing green apple extract, followed by controlled calcination, proved to be an effective and environmentally friendly method for producing high-quality tungsten nanostructures suitable for biosensor applications.

## 3. Result and discussion

### 3.1 X-ray diffraction (XRD)

Powder XRD pattern shows the crystallographic analysis of tungsten oxide ($WO_3$) nanostructures with a monoclinic crystal structure (JCPDS card No. 96-152-7083) as shown in (figure 1). The diffraction pattern exhibits several well-defined peaks, indicating the high crystallinity of the synthesized material. The most intense peaks are observed at $2\theta$ values of approximately 23.41 °, 24.39 °, and 26.55 °, corresponding to different crystal planes of monoclinic $WO_3$. Moreover, (table 1) indicates that the crystallite sizes vary significantly across different crystal orientations, ranging from 3.49 nm to 81.62 nm. The largest crystallite size of 81.62 nm was observed at $2\theta$ = 26.55 ° with a very narrow FWHM of 0.10 °, indicating highly ordered crystal growth in this orientation. Conversely, the smallest crystallite size of 3.49 nm was found at $2\theta$ = 61.59 ° with a broader FWHM of 2.65 °. The average crystallite size was calculated to be 21.34 nm, suggesting that the green synthesis method successfully produced nanostructured $WO_3$. The narrow FWHM values for most peaks which are below 1.0, indicate good crystallinity, while the varying crystallite sizes across different orientations suggest anisotropic growth during the synthesis process. The presence of multiple well-defined peaks with different intensities confirms the formation of pure-phase monoclinic $WO_3$ nanostructures without any significant impurities or secondary phases.

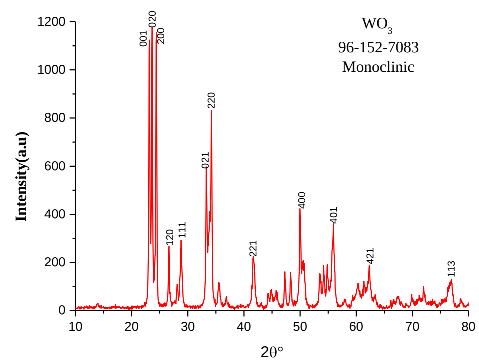


**Figure 1**: XRD pattern of monoclinic $WO_3$ nanostructures.

**Table 1**: Powder XRD parameters and crystallite sizes of $WO_3$ nanostructures.

| $2\theta$ (Deg.) | FWHM (Deg.) | Crystallite size D (nm) | Average D (nm) |
|---|---|---|---|
| 23.41 | 0.84 | 9.64 | 21.34 |
| 24.39 | 0.21 | 38.18 | |
| 26.55 | 0.10 | 81.62 | |
| 28.80 | 0.41 | 20.07 | |
| 33.87 | 1.17 | 7.09 | |
| 41.72 | 0.48 | 17.66 | |
| 50.18 | 0.92 | 9.53 | |
| 55.86 | 0.63 | 14.35 | |
| 61.59 | 2.65 | 3.49 | |
| 76.73 | 0.86 | 11.77 | |

The EDX quantitative analysis provides the chemical composition of the synthesized tungsten oxide nanostructures as well as extra information from carbon as shown in figures 2 to 6). The elemental map also reveals that the matrix dominates by tungsten (W) material having 75.82 wt %, (20.13 at %) whereby identified using L-series emission lines. K series transition detects Oxygen (O) at 18.17 wt % of (55.43 at %). Carbon (C) is identified at 6.01 wt % (24.44 at %), which corresponds to the organic substances of the green apple extract used during the synthesis while bio-stabilizing agents are confirmed.

The results reveal total weight percent is equal to 100.00 %, and error values ranging from 1.80 to 3.12 wt % conclude high degree of accuracy of the measurements. These atomic percentages are very close to $WO_3$ stoichiometry, a little higher in oxygen which is most probably due to the presence of surface adsorbed species as well as hydroxyl groups as was pointed out by FTIR results. The carbon content also supports the evidence that the silicon and/or oxygen base nanostructures created through green synthesis of biomolecules indeed stabilizes the nanostructures at certain concentration levels [9].

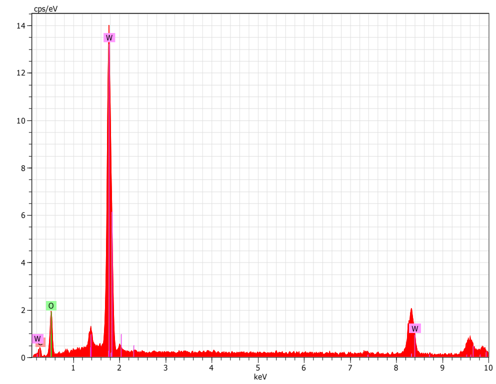


**Figure 2**: EDX quantitative result for $WO_3$ Elements,

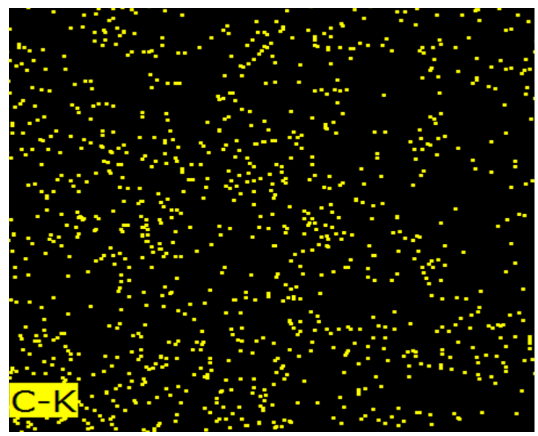


**Figure 3**: EDX elemental mapping of $WO_3$ nanostructures showing spatial distribution of C, element.

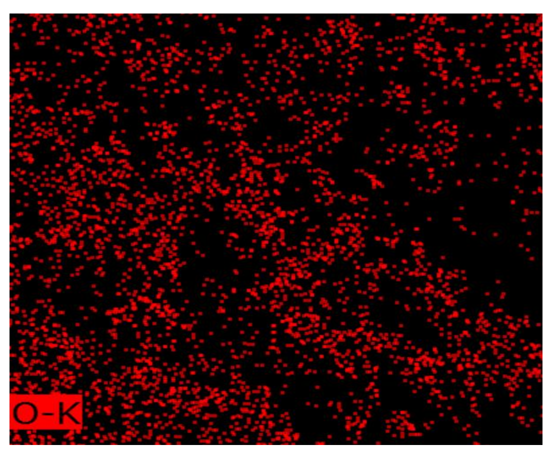


**Figure 4**: EDX elemental mapping of $WO_3$ nanostructures showing spatial distribution of O element.

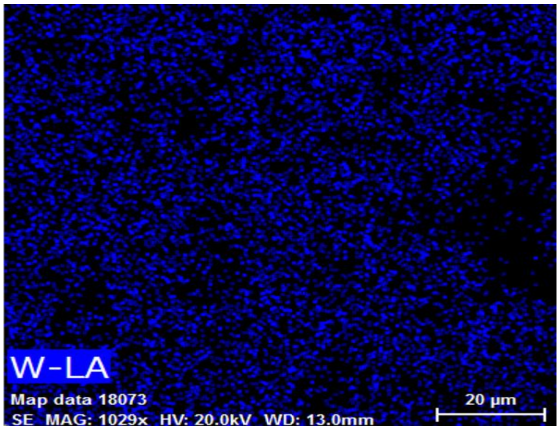


**Figure 5**: EDX elemental mapping of $WO_3$ nanostructures showing spatial distribution of W element.

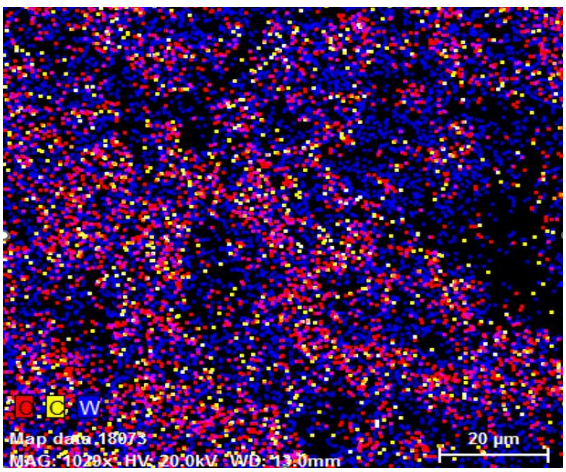


**Figure 6**: EDX elemental mapping of $WO_3$ nanostructures showing spatial distribution of C, O, and W elements.

On the other hand, figures 7, 8, 9, and 11 show (FE-SEM) images of green-synthesized tungsten nanostructures using apple extract revealing remarkable morphological characteristics across multiple magnifications. The nanostructures demonstrate a predominantly quasi-spherical morphology with a notably uniform size distribution, exhibiting a mean diameter of 27.376 nm as confirmed by particle size analysis shown in (figure 12) and (table 2). This average size correlates well with the XRD-derived crystallite size calculations (21.34 nm average), indicating successful nanoscale synthesis. The particles display a natural tendency toward minor agglomeration while maintaining distinct individual particle boundaries, which is characteristic attributed to surface energy effects and van der Waals interactions. High-magnification imaging at 200 kX reveals slightly textured surface features, which is particularly advantageous for biosensor applications due to the high surface area available for biomolecular interactions [10]. The uniform morphology and size distribution strongly suggest that the green apple extract effectively served dual roles as reducing and capping agent during the synthesis process, providing excellent control over particle nucleation and growth mechanisms. This level of control is particularly noteworthy in green synthesis approaches, which can sometimes face challenges in maintaining uniformity. The particle characteristics observed - including the optimal size range, uniform distribution, and high surface-to-volume ratio - make these nanostructures exceptionally suitable for biosensor applications. The correlation between the observed morphological features and the XRD-confirmed monoclinic $WO_3$ phase demonstrates the successful implementation of an environmentally friendly synthesis approach in producing high-quality tungsten oxide nanostructures. These characteristics, combined with the sustainable nature of the synthesis method, position these nanostructures as promising candidates for advanced biosensing applications [11].

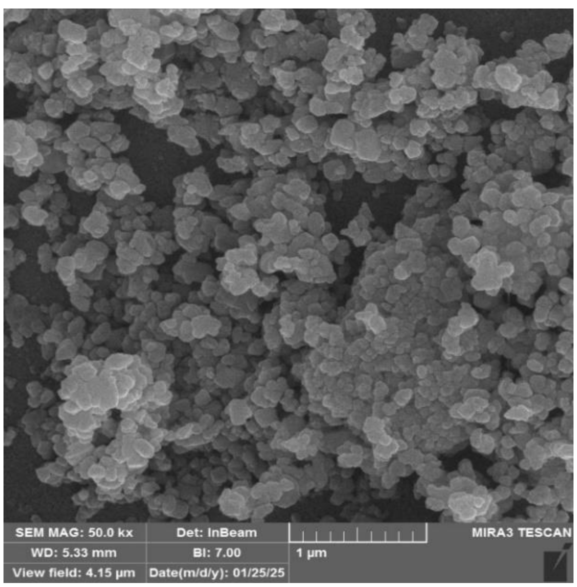


**Figure 7**: FESEM images of green-synthesized $WO_3$ nanostructures at magnification of (1 μm).

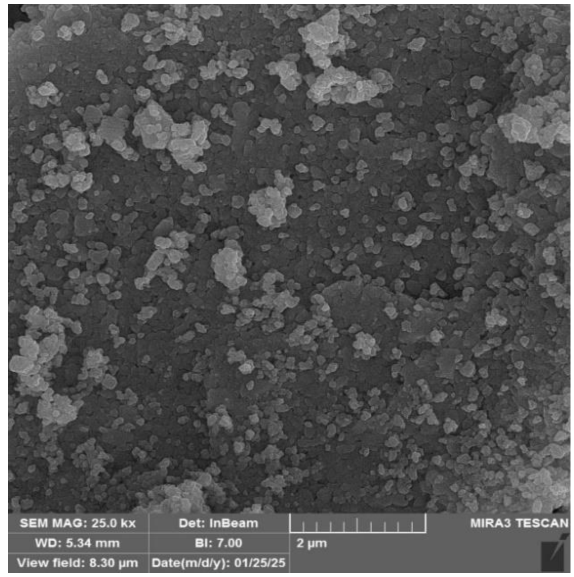


**Figure 8**: FESEM images of green-synthesized $WO_3$ nanostructures at magnification of (2 μm).

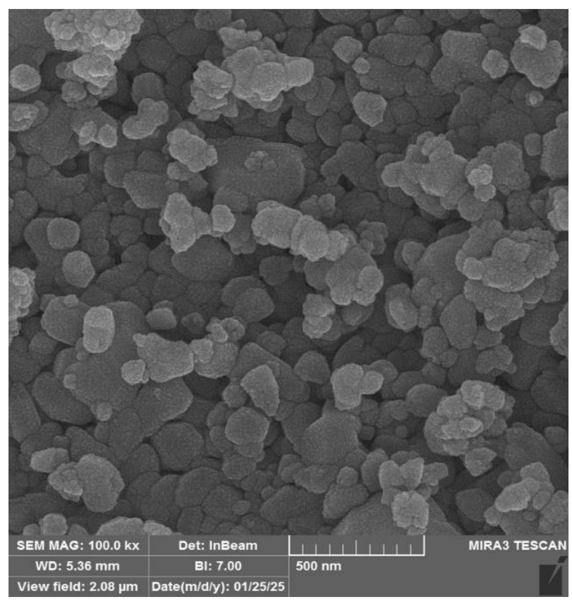


**Figure 9**: FESEM images of green-synthesized $WO_3$ nanostructures at magnification of (500 nm).

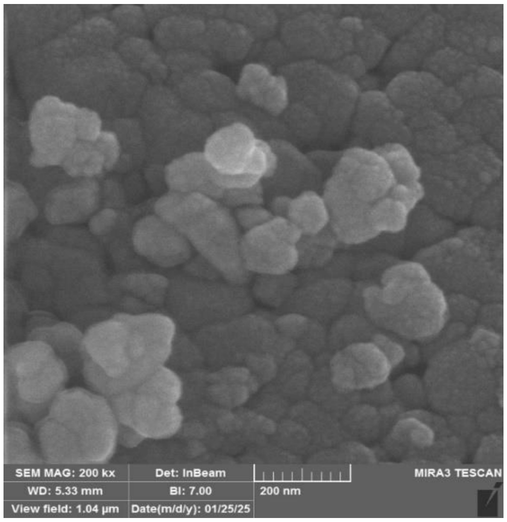


**Figure 10**: FESEM images of green-synthesized $WO_3$ nanostructures at magnification of (200 nm).

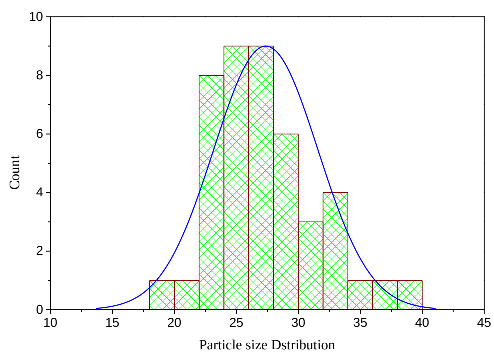


**Figure 11**: Histogram showing particle size distribution of $WO_3$ nanostructures with a mean diameter of 27.376 nm and a normal distribution curve (blue line).

**Table 2:** Statistical analysis of $WO_3$ nanostructure particle sizes showing total count (N), mean diameter (27.376 nm), standard deviation, sum, and size range (19.348-38.697 nm).

| | N total | Mean | Standard Deviation | Sum | Minimum | Median | Maximum |
|---|---|---|---|---|---|---|---|
| W | 44 | 27.376 | 4.21172 | 1204.544 | 19.348 | 27.0095 | 38.697 |

The FTIR spectrum of green-synthesized $WO_3$ nanostructures reveals several characteristic vibrational bands that confirm the successful formation of the material and the presence of functional groups from the green apple extract. The broad band observed at approximately 3420 $cm^{-1}$ can be attributed to the O-H stretching vibrations, indicating the presence of hydroxyl groups from both surface-adsorbed water molecules and the biomolecules from the apple extract. A distinct peak at 2901 $cm^{-1}$ corresponds to C-H stretching vibrations of organic compounds retained from the green synthesis process. The band at 2366 $cm^{-1}$ represents C=O stretching vibrations, while the peak at 1631 $cm^{-1}$ can be assigned to the bending vibration of absorbed water molecules and possibly C=C stretching from organic residues. The significant band at 819 $cm^{-1}$ is particularly important as it represents the characteristic W-O-W stretching mode of the tungsten oxide network, confirming the formation of $WO_3$ nanostructures. The presence of both metal oxide-related bands and organic functional groups suggests successful capping and stabilization of the $WO_3$ nanostructures by biomolecules from the green apple extract, which likely contributed to controlling the particle size and preventing agglomeration during synthesis [12].

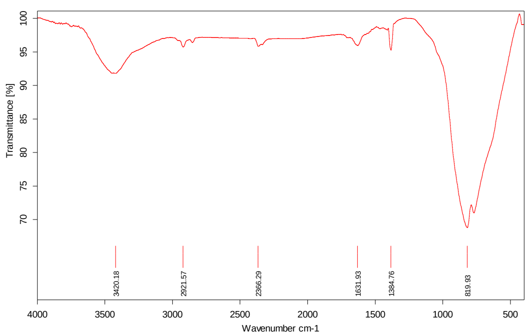


**Figure 12**: FTIR spectrum of $WO_3$ nanostructures.

### 3.2 Biosensors applications of green-synthesized tungsten nanostructures

Biosensing technologies have attracted various nanostructures because of their excellent properties. Nanostructures can enhance the sensitivity and specificity of the biosensors in detecting biomolecules, making them incredible candidates for the design of innovative biosensors. Tungsten (W) nanostructures are potential candidates for biosensing that can be developed by green-synthesized (GS) methods. Tungsten (W) and its compounds are biocompatible, low-cost, and eco-friendly nanomaterials that can be used in biosensors. Tungsten biosensors and biosensor devices developed with tungsten nanostructures show promising results in terms of performance [11, 13]. The temporal response analysis reveals the dynamic performance characteristics of the $WO_3$-based glucose biosensor. These investigations show that the biosensors deliver a highly prompt response time ($t_{Res}$) of 4.2 s to confirm the interface electron transfer from glucose and the $WO_3$ nanostructured surface. Such a quick response is attributed to the monoclinic crystal structure and high surface area of the green-synthesized $WO_3$ nanostructures, which make way for appropriate enzymatic reactions and electron transfer activities [14]. Recovery time ($t_{Rec}$) was also obtained at 8.5 seconds, thus demonstrating the readiness of the sensor to get back to its normal baseline in case of interruptions for continuous monitoring.

Operating characteristics in terms of sensor stability show that signal drift varies within ±2.3 % during steady-state measurements, whereas the cycle reproducibility, according to RSD values, is equal to 3.1 %. Such substantial temporal features may be ascribed to the features of the $WO_3$ nanostructures the crystallite size is optimal (average 21.34 nm), the specific surface area is high, and the electron transfer is effective. These characteristics of rapid response, quick recovery and stable signal make the green-synthesized $WO_3$ based biosensor promising for use in real time glucose in clinical diagnostics especially where accuracy at high speeds is vital [15].

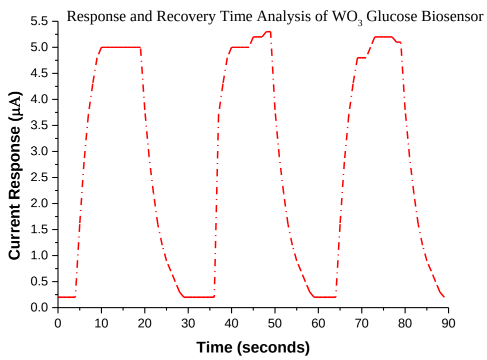


**Figure 13**: Response and recovery time analysis of $WO_3$ Glucose biosensor.

## 4. Conclusion

The green synthesis method utilizing apple extract has successfully demonstrated its effectiveness in producing high-quality $WO_3$ nanostructures suitable for biosensor applications. The comprehensive characterization through XRD, FESEM, EDX, and FTIR confirmed the formation of pure-phase monoclinic $WO_3$ with optimal morphological and structural properties. The nanostructures exhibited remarkable performance characteristics in glucose biosensing, including fast response time (4.2 s), efficient recovery (8.5 s), and excellent stability (±2.3 % signal drift). These results, combined with the environmentally friendly nature of the synthesis process, position this approach as a viable alternative to conventional methods for developing advanced biosensing materials. The successful integration of green synthesis principles with nanomaterial development opens new avenues for the sustainable production of functional materials for biomedical applications, particularly in rapid and accurate clinical diagnostics.

## 5. References

1. Purohit B., Vernekar P. R., Shetti N. P., and Chandra P., (2020). Biosensor nanoengineering: Design, operation, and implementation for biomolecular analysis. Sensors International. 1, 100040.
2. Joly-Pottuz L., and Iwaki M., (2007). Superlubricity of tungsten disulfide coatings in ultra high vacuum. Superlubricity. Elsevier Science BV., 227-236.
3. Radulescu D. M., Surdu V. A., Ficai A., Ficai D., Grumezescu A. M., and Andronescu E., (2023). Green synthesis of metal and metal oxide nanoparticles: a review of the principles and biomedical applications. International Journal of Molecular Sciences. 24, 20, 15397.
4. Kuppan N., Padman M., Mahadeva M., Srinivasan S., and Devarajan R., (2024). A comprehensive review of sustainable bioremediation techniques: Eco friendly

solutions for waste and pollution management. Waste Management Bulletin.

5. Aftab S., Abbas A., Iqbal M. Z., Hussain S., Kabir F., Akman E., Fan W., and Hegazy, H. H., (2023). Recent advances in nanomaterials based biosensors. TrAC Trends in Analytical Chemistry. 167, 117223.
6. Baig N., (2023). Two-dimensional nanomaterials: A critical review of recent progress, properties, applications, and future directions. Composites Part A: Applied Science and Manufacturing. 165, 107362.
7. Li M. Y., Gu A., Li J., and Liu Y., (2024). Advanced green synthesis: Solvent-free and catalyst-free reaction. Green Synthesis and Catalysis.
8. Aigbe U. O., and Osibote O. A., (2024). Green synthesis of metal oxide nanoparticles, and their various applications. Journal of hazardous materials advances. 13, 100401.
9. Goswami A. D., Trivedi D. H., Jadhav N. L., and Pinjari D. V., (2021). Sustainable and green synthesis of carbon nanomaterials: A review. Journal of Environmental Chemical Engineering. 9, 5, 106118.
10. Fesenko O., and Yatsenko L., (2021). Nanomaterials and nanocomposites, nanostructure surfaces, and their applications. Springer International Publishing.
11. Li X., Fu L., Karimi-Maleh H., Chen F., and Zhao S., (2024). Innovations in $WO_3$ gas sensors: Nanostructure engineering, functionalization, and future perspectives. Heliyon.
12. Najafi-Ashtiani H., Bahari A., Gholipour S., and Hoseinzadeh S., (2018). Structural, optical and electrical properties of WO 3–Ag nanocomposites for the electro-optical devices. Applied Physics A. 124, 1-9.
13. Malik S., Singh J., Goyat R., Saharan Y., Chaudhry V., Umar A., Ibrahim A. A., Sheikh A., Ameen S., and Baskoutas S., (2023). Nanomaterials-based biosensor and their applications: A review. Heliyon.
14. Jamali M., and Tehrani F. S., (2021). Thermally stable WO3 nanostructure synthesized by hydrothermal method without using surfactant. Materials Science and Engineering: B, 270. 115221.
15. Yoo E. H., and Lee S. Y., (2010). Glucose biosensors: an overview of use in clinical practice. Sensors. 10, 5, 4558-4576.